Stochastic modelling of insulin sensitivity and adaptive glycemic control for critical care

Jessica Lin[a,*], Dominic Lee[b], J. Geoffrey Chase[a], Geoffrey M. Shaw[c,d], Aaron Le Compte[a], Thomas Lotz[a], Jason Wong[a], Timothy Lonergan[a], Christopher E. Hann[a]

[a] Department of Mechanical Engineering, Centre for Bio-Engineering, University of Canterbury,
Private Bag 4800, Christchurch, New Zealand
[b] Department of Mathematics and Statistics, University of Canterbury, Private Bag 4800, Christchurch, New Zealand
[c] University of Otago, Christchurch School of Medicine and Health Sciences, Christchurch, New Zealand
[d] Canterbury District Health Board, Department of Intensive Care Medicine, Christchurch Hospital, New Zealand

ARTICLE INFO

ABSTRACT

Targeted, tight model-based glycemic control in critical care patients that can reduce mortality 18–45% is enabled by prediction of insulin sensitivity, S_I. However, this parameter can vary significantly over a given hour in the critically ill as their condition evolves. A stochastic model of S_I variability is constructed using data from 165 critical care patients. Given S_I for an hour, the stochastic model returns the probability density function of S_I for the next hour. Consequently, the glycemic distribution following a known intervention can be derived, enabling pre-determined likelihoods of the result and more accurate control.

Cross validation of the S_I variability model shows that 86.6% of the blood glucose measurements are within the 0.90 probability interval, and 54.0% are within the interquartile interval. "Virtual Patients" with S_I behaving to the overall S_I variability model achieved similar predictive performance in simulated trials (86.8% and 45.7%). Finally, adaptive control method incorporating S_I variability is shown to produce improved glycemic control in simulated trials compared to current clinical results. The validated stochastic model and methods provide a platform for developing advanced glycemic control methods addressing critical care variability.

1. Introduction

Critically ill patients often experience stress-induced hyperglycemia and high levels of insulin resistance [1–4]. The increased counter-regulatory hormone and cytokine response stimulates endogenous glucose production and increases effective insulin resistance. Absolute and relative insulin deficiency and steroid-based therapies are further causes. The metabolic response to stress is characterised by highly variable changes in insulin sensitivity and glucose metabolism. The overall result is hyperglycemia, the pathogenesis of which is becoming well described [1,5]. Tight glucose control has been shown to reduce Intensive Care Unit (ICU) patient mortality up to 45%.

Previous clinical model-based glycemic control studies include [6–12]. Chase et al. [10] and Plank et al. [8] developed highly adaptive, clinically verified, targeted control algorithms. Following [10], the specialized relative insulin and nutrition tables (SPRINT) protocol [7,11] was developed to simplify critical care implementation. Over 165 patients and

23,000 patient hours, it achieved an average blood glucose level of 5.8 ± 1.2 mmol/L with 61% of the time in the 4–6.1 mmol/L band [4]. This is the only approach adaptive to insulin sensitivity variation, as reflected in the hour to hour insulin-nutrition response to changing blood glucose levels.

A common risk in intensive insulin therapy is hypoglycemia. Many current ad hoc intensive insulin therapy protocols have reported hypoglycemic episodes for up to 25% of patients [3,13]. Therefore, understanding and modelling the variability in insulin sensitivity can assist clinical control intervention and minimise associated risk.

Currently, no intensive insulin therapy protocol offers the glycemic response likelihood to an intervention. Clinicians are thus partly blind in controlling this highly dynamic system. Therefore, the goal of this study is to produce blood glucose probability distributions for control intervention decisions based on stochastic models of clinically observed parameter variations. The result will allow more accurately targeted control, with user specified likelihood on the glycemic response.

2. Glucose–insulin system model and parameter identification

A clinically verified patient-specific glucose–insulin metabolic model [10,12,14,15] is used to account for time-varying insulin sensitivity in critical care.

2.1. Glucose–insulin system model

The glucose–insulin system model is presented in Eqs. (1)–(5):

$$\dot{G} = -p_G G - S_I(G + G_E)\frac{Q}{1 + \alpha_G Q} + P(t) \tag{1}$$

$$\dot{Q} = -kQ + kI \tag{2}$$

$$\dot{I} = -n\frac{I}{1 + \alpha_I I} + \frac{u_{ex}(t)}{V_I} \tag{3}$$

$$P(t_i < t < t_{i+1}) = \bar{P}_{i+1} + (P(t_i) - \bar{P}_{i+1})\,e^{-k_{pd}(t-t_i)} \quad \text{where} \quad \bar{P}_{i+1} < P(t_i) \tag{4}$$

$$P(t_i < t < t_{i+1}) = \bar{P}_{i+1} + (P(t_i) - \bar{P}_{i+1})\,e^{-k_{pr}(t-t_i)} \quad \text{where} \quad \bar{P}_{i+1} > P(t_i) \tag{5}$$

where G (mmol/L) denotes glucose above an equilibrium level G_E (mmol/L), and I (mU/L) denotes the plasma insulin from an exogenous insulin input. Insulin utilization over time is captured by Q (mU/L), where k (1/min) is the effective insulin half-life parameter. Patient endogenous glucose removal and insulin sensitivity are p_G (1/min) and S_I (L/mU min), respectively. The parameter V_I (L) is the insulin distribution volume and n (1/min) is the first order decay rate for plasma insulin. External nutrition and insulin inputs are $P(t)$ (mmol/L min) and $u_{ex}(t)$ (mU/min), respectively. Michaelis–Menten parameters α_I (L/mU) and α_G (L/mU) define plasma insulin disappearance saturation and insulin-stimulated glucose removal saturation,

respectively. The exogenous glucose appearance and decay rate used to define $P(t)$ are k_{pr} and k_{pd} Specific details on physiological model dynamics are evaluated in [10,12,16].

In Eq. (1), the saturation mechanism on insulin effect creates a unique index of insulin sensitivity, S_I, compared to other model-based measures. The result is an S_I index that more closely approximates the effective net tissue sensitivity to insulin, and its variation to the evolution of patient condition and drug therapy. It has also been shown to drive patient response to intervention and thus control efficacy in prior studies [10,12]. This model measure is also highly correlated to clamp-derived ISI over 146 patients [17–19]. Hence, understanding variation in S_I should enable more effective control.

2.2. Integral-based parameter identification

Identifying insulin sensitivity has been extensively studied [1,20]. Using constant population values for p_G, α_G, α_I, n, k and V_I [15] limits the model unknowns in this case to S_I. This study utilizes an integration-based parameter identification method first presented in Hann et al. [15]. Constraints are placed on S_I to ensure it is within a physiologically valid range.

3. Stochastic modelling and validation

The control algorithms of [10,12] calculate the interventions necessary for targeted glycemic regulation by assuming that the currently identified S_I values are constant between the control intervention and the one-hour time interval to achieve a preselected target at the next measurement. This assumption is made due to lack of better knowledge. However, S_I can evolve significantly [15], and sudden variations may occur due to the onset of acute conditions [12].

The ultimate goal is to produce blood glucose probability bands for a given intervention based on clinically observed parameter variations using an ICU population based stochastic model. Such bands would allow glycemic target selection with guaranteed levels of certainty that a result will meet or exceed a given glycemic level. Such a model would also identify outlying measurements to a pre-defined probability level.

An initial such model was developed using data from 18 critical care patients in the Department of Intensive Care Medicine (ICU), Christchurch Hospital [21]. It was clinically verified with data from 8 independent critical care glycemic control trials. The model successfully captured the identified S_I variation trend, accounting for 84% of measurements within the 0.90 probability interval, and 45% within the interquartile interval. However, it was limited in its formulation from a population limited in size ($n = 18$), the resulting level and variety of critical illness, and the glucose data density (1–4 hourly).

Between July 2005 and June 2006, 165 patients were put on the SPRINT protocol in the Christchurch Hospital ICU [11]. A new stochastic model was created using data from these 165 controlled patients, totalling over 23,000 h, to better represent stochastic S_I variation in critical care. By comparison, the initial model was only built on close to 1300 h of data over 18 patients, none of whom were on intensive glycemic control. The SPRINT blood glucose data were primarily hourly data,

Table 1 – Clinical SPRINT cohort information

|	All	Length of stay ≥ 3 days
Number of patients	165	120
Age (years)	65 [50–74]	65 [49–74]
% Male	66%	66%
APACHE II score	19 [15–25]	19 [15–26]
APACHE II risk of death	29% [15–55%]	31% [16–56%]

whereas the previous model was built from 3–4 hourly data. Therefore, SPRINT data provides a better view of the highly dynamic critically ill condition that is more suitable for intensive glycemic control.

3.1. Stochastic S_I model for critical care

Patient specific insulin sensitivity parameter profiles, S_I, are fitted hourly to the 165 SPRINT patients. Table 1 shows the patient data. Glycemic control had greatest effect for those with greater than 3-day stay [3,13] and they make up 73% of this cohort and 96% of the patient hours.

Fitted S_I is constrained between physiological limits of 1×10^{-5} mU/L min and 1×10^{-3} mU/L min [22,23]. A two-dimensional kernel density estimation method is used to construct the stochastic S_I model that describes the hourly transition of parameter values. The method has the advantage of producing a smooth, continuous function across the parameter range [24]. The overall result is a bivariate probability density function for the potential parameter values. Fig. 1 shows the distribution of fitted hour to hour S_I and the two-dimensional kernel joint probability density.

The two-dimensional kernel density method is chosen for creating the stochastic model because the distribution of S_I at hour $n+1$ ($S_{I,n+1}$) varies with S_I at hour n ($S_{I,n}$), and cannot be simply described with a standard statistical distribution. Thus, the variations in S_I can be treated as a Markov process.
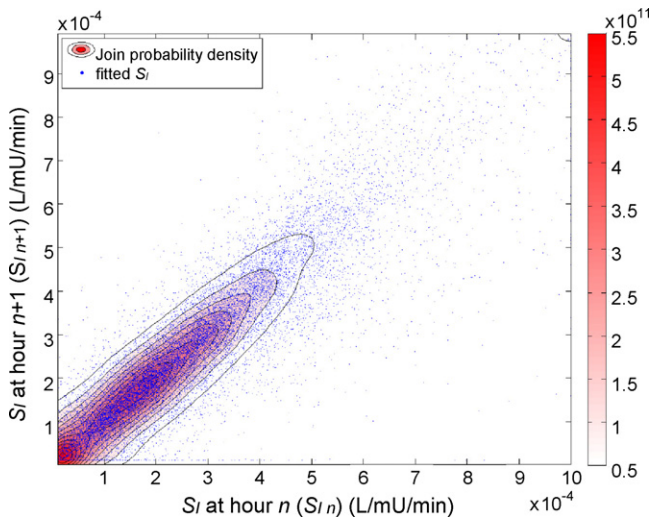
Fig. 1 – Fitted hourly S_I variation (dots) and joint kernel probability density (shaded contours). The area under the joint probability density function surface in the model space sums to 1.0.

A Markov process has the property that the conditional probability density function of future states of the process, given the present state, depends only upon the current state. Therefore, using the Markov property of the stochastic behaviour of S_I, the conditional probability density of $S_{I,n+1}$ taking on a value y can be calculated by knowing $S_{I,n} = x$:

$$P(S_{I,n+1} = y | S_{I,n} = x) = \frac{p(S_{I,n} = x, S_{I,n+1} = y)}{p(S_{I,n} = x)} \tag{6}$$

Considering the fitted S_I in a 2D space, as shown in Fig. 1, the joint probability density function across the x–y ($S_{I,n} - S_{I,n+1}$) plane is defined by the fitted values shown by the dots whose coordinates are x_i and y_i:

$$p(x, y) = \frac{1}{n} \sum_{i=1}^{n} \frac{\phi(x; x_i, \sigma_{x_i}^2)}{p_{x_i}} \frac{\phi(y; y_i, \sigma_{y_i}^2)}{p_{y_i}} \tag{7}$$

$$p_{x_i} = \int_0^\infty \phi(x; x_i, \sigma_{x_i}^2) \tag{8}$$

$$p_{y_i} = \int_0^\infty \phi(y; y_i, \sigma_{y_i}^2) \tag{9}$$

Effectively, the 2D joint probability density function is the normalised summation of normal probability density functions $\phi(x; x_i, \sigma_{x_i}^2)$ centred at individual data points.

In Eqs. (7)–(9), the variance, σ, at each data point is a function of the local data density in a centred and orthonormalised space of x and y. Putting Eqs. (8) and (9) into Eq. (7) normalises each $\phi(x; x_i, \sigma_{x_i}^2)$ and $\phi(y; y_i, \sigma_{y_i}^2)$ in the positive domain, effectively putting boundaries along $x = 0$ and $y = 0$, and enforcing physiological validity in S_I values.

In Eq. (6), the right hand side denominator can be calculated by integrating Eq. (7) with respect to y. Hence, Eq. (7) can be calculated:

$$p(S_{I,n+1} = y | S_{I,n} = x) = \sum_{i=1}^{n} \omega_i(x) \frac{\phi(y; y_i, \sigma_{y_i}^2)}{p_{y_i}} \tag{10}$$

$$\omega_i(x) = \frac{\phi(x; x_i, \sigma_{x_i}^2)/p_{x_i}}{\sum_{j=1}^{n} \phi(x; x_j, \sigma_{x_j}^2)/p_{x_j}} \tag{11}$$
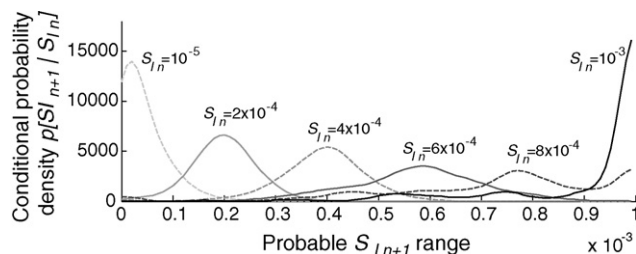
Thus, knowing $S_{I,n} = x$ at hour n, the probability of $S_{I,n+1} = y$ at hour $n+1$ can be calculated using Eqs. (10) and (11). Plotting Eq. (10) across the x–y ($S_{I,n} - S_{I,n+1}$) plane, the resulting 3-D stochastic model is shown in Fig. 2. This essentially creates an approximation to the parameter variation behaviour according to how the existing data behaves. Where there is higher density of data, more certainty can be drawn on the "true" behavioural pattern. With this stochastic model, given a current identified S_I value, the probability density can be calculated across the possible range of S_I values for the coming hour. The probability is conditional because the probability density for a coming hour is dependent on the identified current hourly S_I.
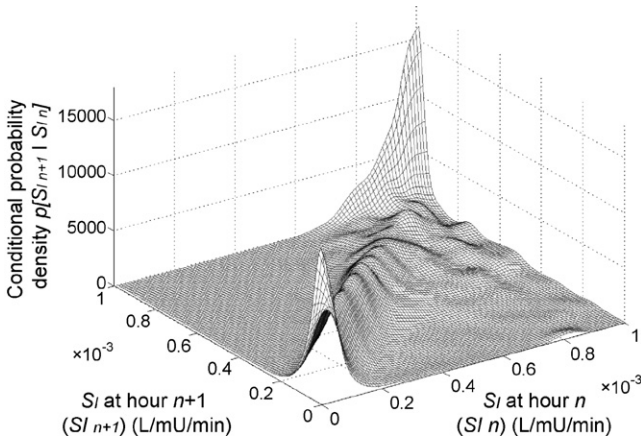
Fig. 2 – Stochastic model of S_I variability. Conditional probability density functions are the surface slices along $S_{I,n+1}$ axis, each slice has an area under the curve summing to 1.0.

Across the fitted range of S_I, the conditional probability density function is largely uni-modal and symmetric. However, as shown in the cascade plot of conditional $S_{I,n+1}$ probability density functions across the $S_{I,n}$ model range in Fig. 3, there are some numerical artefacts near the boundaries of the fitted range. Probability density functions for $S_{I,n}$ peak at boundary values because of the fitting constraints. For $S_{I,n} = [1 \times 10^{-5}, 1 \times 10^{-4}]$ and $[0.75 \times 10^{-3}, 1 \times 10^{-3}]$ at the edges of Fig. 3, the percentile values away from the median do not necessarily decrease in probability. These ranges span 34% of the fitting range $[1 \times 10^{-5}, 1 \times 10^{-3}]$, in which 20% of the SPRINT data falls (18% between $S_{I,n} = [1 \times 10^{-5}, 1 \times 10^{-4}]$ and 2% between $[0.75 \times 10^{-3}, 1 \times 10^{-3}]$ in Fig. 1). Note that Figs. 2 and 3 show the conditional probability density functions which are scaled to have the area under each function summing to 1. Thus, the asymmetry becomes very pronounced in Figs. 2 and 3. The probability of S_I taking on these asymmetric conditional probability density functions is in fact very low in the overall joint probability density function shown in Fig. 1, where the probability density sums to 1 over the entire fitting surface.

The asymmetric S_I probability density functions could perhaps be due to other not explicitly modelled physiology, such as variations in endogenous glucose production. More specifically, "bumpy" areas of S_I probability density function in Fig. 3 may be a sign of S_I absorbing physiology unmodelled or undermodelled in Eqs. (1)–(5). However, this unmodelled phys-

iology represents uncommon sudden, or extreme, dynamics, evident by the low overall joint probability density in these areas in Fig. 1. Practically, to include all such variations in the glucose–insulin model would make it overly complicated and it would thus lose clinical feasibility. Such additions would also require added assumptions for endogenous insulin or glucose production that are not clinically measured in real-time.

Assumptions for these responses could also compromise control accuracy, as both endogenous insulin and glucose productions are known to vary significantly between patients [25–29] and over time. In addition, endogenous glucose production is suppressed with significant insulin administration in both normal and stressed states [30], which is the case for critically ill patients under insulin therapy for glycemic management. Similarly, the endogenous insulin production is effectively removed or significantly reduced in the presence of significant exogenous insulin [29,31–33], not to mention its inhibition in stress hyperglycemia (e.g. [34]). It is therefore, in the interest of this model-based clinical control applications, to have these effects mitigated into S_I. In Refs. [10,12,15], the model of Eqs. (1)–(5) and the impact of mitigated effects are discussed in detail. The result is a much more clinically feasible control model, where S_I accounts for critically ill population's overall sensitivity to insulin and/or its utilisation.

In Fig. 1, the lower bound for S_I has greater influence on the overall stochastic model than the upper bound. However, no patients have fitted S_I staying at the lower bound for a prolonged period, again suggesting that these occasions are more sudden, short term condition, such as suppressed insulin sensitivity or utilisation due to drug therapies, rather than long term, or gradual changes, such as increased glucose production. During numerical fitting, if fitted S_I stays at the lower bound for a prolonged period of 5 h, the fitting method recognises a gradual evolution, and adjusts G_E to address factors such as endogenous glucose production. During the total of 23,324 control hours, only 39 such occurrences were observed, which is 0.85% of the time.

The short term changes, although causing fitted S_I to hit the lower bound, if unconstrained will often result in negative S_I because of significant drug effects or acute medical conditions such as atrial fibrillation [12]. In addition, increased endogenous insulin production with inhibited glucose production can result in an effectively zero or negative modelled S_I. These cases are too wide ranged to be accounted for in the physiological model. Note that an evolving G_E that is too high leads to a reduction in modelled endogenous glucose production, and a higher S_I may also result in the model due to a lower $-p_G G$ term. Mitigating the impact of these events into fitted S_I simplifies the model to be feasible for clinical control.

In addition, incorrect modelling of these conditions which are difficult to account for can severely compromise patient safety. More specifically, underestimating S_I can lead to excess insulin being given. With the aim of applying the physiological and stochastic models in clinical control, the lower bound of S_I has an important role. Finally, the fitted S_I, with higher data concentration around the lower bound, realistically reflects the highly variable dynamics in the critical care environment, where drug therapies and acute medical conditions that result in highly resistant patients are common.

Fig. 3 – Cascade of S_I probability density function slices over the fitted S_I range.
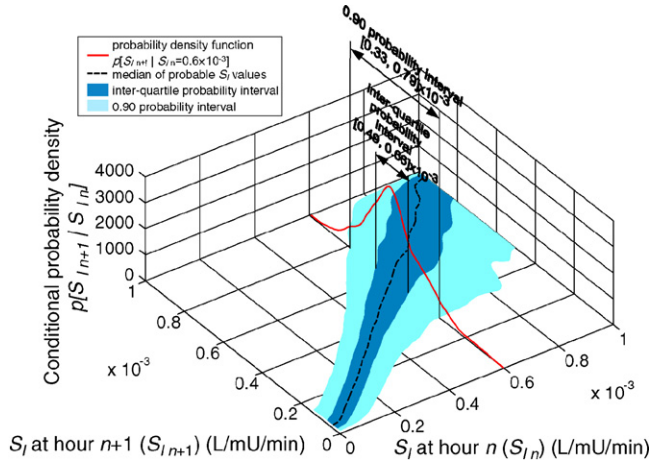
Fig. 4 – Probability density function of potential S_I. Probability intervals across the model space from Fig. 2 are shown by shaded areas.

3.2. Clinical implementation and use

Having constructed the S_I stochastic model, the surface of Fig. 2 can be used in a look-up table. Given a clinically identified S_I [10,12], the probability density, and hence the probability intervals, can be obtained, as demonstrated in Fig. 4. The solid 3D line is the kernel density estimate sliced along $S_{I,n} = 0.6 \times 10^{-3}$. This line represents the probability density for potential $S_{I,n+1}$, one hour after having identified the current hour $S_{I,n} = 0.6 \times 10^{-3}$. From this density function, probability intervals are also obtained, giving a median probable S_I value in an hour of 0.58×10^{-3}, interquartile range [0.49×10^{-3}, 0.66×10^{-3}], and the 0.90 probability interval [0.33×10^{-3}, 0.79×10^{-3}].

The probability intervals used here for clinical decision-making, as shown in Fig. 4, are equal-tailed. "Equal-tailed" means that the 0.90 probability interval is between the 5th percentile and the 95th percentile in the probability density function. Equal-tailed probability intervals are based on the assumption and observation that the probability density function is (largely) uni-modal and symmetric. Thus, the values outside the interval are assumed to have lower probability of occurring than the values within the interval and represent "tails" of that distribution.

3.2.1. Probability interval calculation

Using the equal-tailed probability interval boundary values for S_I in Eqs. (1)–(5), the corresponding probability intervals in blood glucose levels for a given intervention from current state can be calculated. This statistical approach holds for any strictly monotone physiological systems [35]. More specifically, in this case, a higher S_I value always produces lower blood glucose than a lower S_I value for a given input and state over the time S_I is defined.

In the cascade plot of the conditional $S_{I,n+1}$ probability density functions across the $S_{I,n}$ range in Fig. 3, it is evident that the assumption that the conditional probability density function is largely uni-modal and symmetric is true for the bulk of the fitted S_I range, but does not hold near the boundaries.

Therefore, in these regions, equal-tailed probability intervals may not give an exact representation of the probability intervals. More simply, the 5th and the 95th percentile in the resulting blood glucose level probability distribution may not contain the exact 90% most probable blood glucose levels. In particular, due to the asymmetric boundary density functions in S_I, blood glucose levels outside this range may have a higher probability density than parts within the 0.90 probability interval.

To exactly obtain the probability density in blood glucose resulting from a known probability density function in S_I, Monte Carlo simulation is the only method. In particular, while the percentile values in S_I correspond to percentile values in blood glucose levels, the "rank" of probability does not [35].

This situation is illustrated in Fig. 5, where the left hand side and right hand side demonstrate the difference between the 0.90 equal-tailed blood glucose probability intervals and the exact probability intervals generated from Monte Carlo simulations. Panels A and B display the same probability density function (pdf) (right axis) and the cumulative distribution functions (cdf) (left axis) in $S_{I,n+1}$, when $S_{I,n} = 8 \times 10^{-4}$ is known. Panels C and D show the resulting pdf (right axis) and cdf (left axis) in blood glucose levels at hour $n+1$ (BG_{n+1}, mmol/L) through Monte Carlo Simulation of the model in Eqs. (1)–(5). The pdf and cdf shown in panels C and D are identical and are the exact solution for the BG_{n+1} probability density function given $S_{I,n} = 8 \times 10^{-4}$. Note that in panels A and B, the x-axes are decreasing from left to right, producing a similar shaped probability density function in blood glucose levels in panels C and D with blood glucose levels increasing as $S_{I,n+1}$ decreases.

The left hand side of Fig. 5, panels A and C illustrate how equal-tailed probability intervals in $S_{I,n+1}$ are translated into the equal-tailed probability intervals in BG_{n+1}. Let f be the transformation function between $S_{I,n+1}$ to BG_{n+1}, which is the physiological model shown in Eqs. (1)–(5), then

$$BG_{100\text{-percentile}} = f(S_{I\,\text{percentile}}) \tag{12}$$

Thus, the percentile values of $S_{I,n+1}$ in panel A corresponds to the reversed (100-percentile) values in BG_{n+1} in panel C. Or more simply, solving Eqs. (1)–(5) using the 5th percentile value in $S_{I,n}$ produces the 95th percentile blood glucose levels, $BG_{95} = f(S_{I5})$ given that f is strictly monotone [35]. Therefore, the $S_{I,n+1}$ probability interval between the 5th and the 95th percentile ($S_{I,n+1} = [0.33 \times 10^{-3}, 0.98 \times 10^{-3}]$ between ▷ and ◁ in panel A) consequently gives the BG_{n+1} probability interval between the 5th and the 95th percentile ($BG_{n+1} = [1.9, 5.4]$ between ▷ and ◁ in panel C). More simply, as shown in the left hand side of Fig. 5,

- Equal-tailed 0.90 probability interval in $S_{I,n+1} = [S_{I5}, S_{I95}]$.
- Equal-tailed 0.90 probability interval in $BG_{n+1} = [f(S_{I95}), f(S_{I5})]$.

However, as illustrated in panel C, the BG_{n+1} probability interval between the 5th and the 95th percentile (▷ and ◁) includes values that have lower probability density than some BG_{n+1} values outside this interval. More specifically, ▷ has lower probability density than the region to its left. This higher probability density region outside the 5–95% range is very narrow and at the very extreme end.
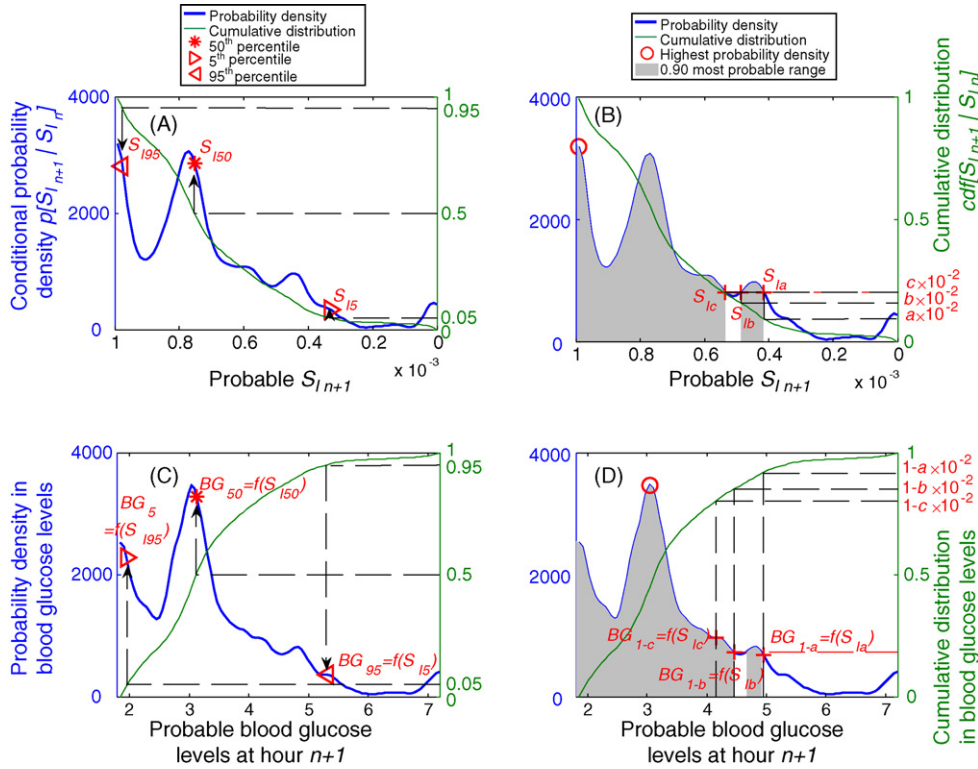
Fig. 5 – Probability density transition from S_I to blood glucose levels. Panels A and B show the pdf (right axis) and the cdf (left axis) in $S_{I,n+1}$, when $S_{I,n} = 8 \times 10^{-4}$ is known. Panels C and D show the resulting pdf (right axis) and cdf (left axis) in blood glucose levels at hour $n+1$ (BG_{n+1}, mmol/L) through Monte Carlo Simulation. The transformation through Eqs. (1)–(5) from upper panels to lower panels is denoted by f. The shaded areas in panel B and D have the highest 90% probability. The 90% most probable $S_{I,n+1}$ intervals in panel B are between cdf = $[a \times 10^{-2}, b \times 10^{-2}]$ and $[c \times 10^{-2}, 1.0]$. Note that higher S_I values in the left hand side of the reversed x-axis in panels A and B results in higher BG values on the right hand side in panels C and D.

On the right hand side of Fig. 5, the 90% most probable $S_{I,n+1}$ values are identified by the shaded areas in panel B. These values are discontinuous, and have higher probability of occurring than values outside the shaded areas. However, taking the boundary values for the 90% most probable $S_{I,n+1}$ values then putting them into Eqs. (1)–(5) does not provide the 90% most probable BG_{n+1} intervals. More simply, as shown in the right hand side of Fig. 5:

- Exact 0.90 probability interval in $S_{I,n+1}$ = shaded intervals in panel B = $[S_{Ia}, S_{Ib}]$ and $[S_{Ic}, S_{I,100}]$, where a, b and c are percentile values of S_{Ia}, S_{Ib} and S_{Ic}, and

$$pdf(S_{Ia}) = pdf(S_{Ib}) = pdf(S_{Ic}) \qquad (13)$$

$$cdf(S_{Ik}) = k \quad \text{for} \ k = a, b, c \qquad (14)$$

$$(100 - c) + (b - a) = 90 \qquad (15)$$

- Exact 0.90 probability interval in BG_{n+1} = shaded intervals in panel D $\neq [f(S_{I100}), f(S_{Ic})]$ and $[f(S_{Ib}), f(S_{Ia})]$, or

$$pdf(f(S_{Ia})) \neq pdf(f(S_{Ib})) \neq pdf(f(S_{Ic})) \qquad (16)$$

Consequently, to obtain the exact probability intervals in BG_{n+1}, Monte Carlo simulations using a minimum of 10,000 $S_{I,n+1}$ values needs to be done to achieve an accuracy of 1%. While such a Monte Carlo simulation can provide the appropriate probability density in BG_{n+1}, it is too computationally expensive to generate useful and effective probability intervals quickly enough for clinical decision support.

3.2.2. Clinical feasibility

An estimated computational comparison between calculating the equal-tailed and the exact probability intervals is summarised in Table 2. The computational timeframe for calculating the exact probability interval is clearly not currently feasible for this type of real-time clinical control. In conclusion, assuming equal-tailed probability intervals provides fast, clinically viable and slightly conservative estimates for the most likely ranges of BG_{n+1}. Therefore, it should not compromise patient safety when used to assist clinical decision-making. As the example in Fig. 5 shows, the 0.90 equal-tailed probability interval in BG_{n+1} ([1.9, 5.4]) covers most of the exact 0.90 most probable range ([1.8, 4.5] and [4.7, 4.9]), providing an effective and clinically useful estimate with far less effort.

3.3. Cross validation

The stochastic S_I model can be integrated into the system model of Eqs. (1)–(5) for use in control. This step allows the blood glucose level probability intervals one hour following an insulin and/or nutrition intervention to be found directly based on the probability density function of $S_{I,n+1}$. Cross validation is used in this study to test the generality of the SPRINT cohort and resulting stochastic model.

For cross validation, the 165 patients are divided into five random groups. Each group has comparable medical conditions, sex, age, and APACHE (Acute Physiology and Chronic Health Evaluation) scores. Five stochastic S_I models are then built, each one using fitted S_I data from four out of five groups. Each stochastic model is then evaluated against the group that is not used for creating the model. Thus, a stochastic model created from groups 1–4 is evaluated against a patient in group 5 in the following steps:

1. At hour 0, the patient's identified S_I is $S_{I,0}$. The stochastic model then produces the 5th, 25th, 75th and 95th percentiles for probable S_I at hour 1, denote $S_{I,1-5}$, $S_{I,1-25}$, $S_{I,1-75}$ and $S_{I,1-95}$.
2. Examine if the identified $S_{I,1}$ is within the inter-quartile probability interval between $S_{I,1-25}$ and $S_{I,1-75}$, and the equal-tailed 0.90 probability interval between $S_{I,1-5}$ and $S_{I,1-95}$.
3. Repeat the process from hour 1 until the end of the patient data.

3.4. Further model applications: virtual patients and trial simulations

A generic stochastic model is built using all 165 SPRINT patients. Incorporating this stochastic model into the

glucose–insulin system model presented in Eqs. (1)–(5), typical critical care patient dynamics can be reproduced numerically given initial conditions in G, Q and I, starting dextrose and insulin inputs, and a starting S_I value.

3.4.1. Virtual patient generation and trial implementation

To generate a "virtual patient" cohort similar to the SPRINT cohort, and therefore representative of a critically ill population, initial conditions to Eqs. (1)–(5) are generated to approximate the statistical distribution of these parameters, as recorded from the SPRINT cohort. Initial S_I values are randomly selected from the initial values fitted from the SPRINT S_I data. Trial lengths were also randomly generated to create a similar statistical distribution to that in the SPRINT trials. Profiles of S_I are then generated using the stochastic model. Using these profiles in Eqs. (1)–(5), "virtual patients" are created that (statistically) approximate the SPRINT cohort on which the model was created, providing a platform for clinical trial simulation and control development. A virtual control trial simulation consists of hourly cycles of the following steps:

1. Generate an hourly $S_{I,n+1}$ value from the stochastic model defined probability density function of the previous hourly S_I value $S_{I,n}$.
2. Generate the end-of-hour virtual blood glucose level using the generated $S_{I,n+1}$ and the specified control (insulin and nutrition) interventions at hour $n+1$ in Eqs. (1)–(5). Standard Glucocard™ blood glucose measurement error [36] is numerically added to the generated blood glucose level, matching the clinical conditions in Christchurch Hospital ICU [12,37].
3. A new S_I, denoted S_I', is fit to the blood glucose levels including random noise that are "measured" during hour $n+1$. Integral-based parameter identification is used to identify S_I' [12,15].
4. The median and equal-tailed 0.90 and inter-quartile probability intervals of potential S_I are generated from the identified S_I' obtained from step 3, using the value of S_I' in the stochastic model as described in Fig. 4.
5. Interventions are determined that position the median glucose and probability intervals to criterion defined by the control algorithm.
6. Return to step 1 with $S_{I,n+1}$ being the new $S_{I,n}$.

Essentially, a virtual patient's S_I evolution follows the joint probability density contour in Fig. 1, making its way to the highest probability density regions. Each $S_{I,n+1}$ is dependent on the previous state, $S_{I,n}$, where the probability density function of of $S_{I,n+1}$ is defined in Eqs. (10) and (11). Hence, in step 1 above, S_I takes a walk to a point, say y, along the probability density function curve $p(S_{I,n+1} = y | S_{I,n} = x)$ as shown in Fig. 4. Step 6 then "walk" the S_I across (along $S_{I,n+1}$ axis) to where $S_{I,n} = y$, and the process repeats.

3.4.2. Virtual trial control algorithm

The control algorithm used in this study is a target-shooting algorithm that probabilistically minimises the risk of hypoglycemia. Interventions include insulin bolus injections, and

Table 2 – Comparison between probability interval computational cost	
0.90 probability interval calculation	
Equal-tailed	Calculation time
Steps	
(1) Calculate the 5th and 95th percentiles in $S_{I,n+1}$ S_{I5} and S_{I95}	~0 s
(2). Equal-tailed 0.90 probability interval in $BG_{n+1} = [f(S_{I95}), f(S_{I5})]$	1 s
Total time	~1 s
0.90 probability interval calculation	
Exact	Calculation time
Steps	
(1) Generate 10,000 $S_{I,n+1}$ using the derived pdf from the stochastic model	2 s
(2) Calculate BG_{n+1} for each of the 10,000 $S_{I,n+1}$ values	5000 s = 83 min
(3) Sort the 10,000 BG_{n+1} values and find the 5th and 95th percentiles	1 s
Total time	~83 min

Table 3 – Sub-cohorts of 165 SPRINT patients for cross validation

Group	No. of patients	Age (year)	Gender (% male) (%)	Average blood glucose level (mmol/L)	Length of trial (h)	Time in 4–6.1 mmol/L band (%)
1	33	57.4 (19.4)	69.7	6.2 (1.9)	144.6 (189.1)	58.1 (24.5)
2	33	66.5 (13.8)	63.6	5.9 (0.7)	141.1 (167.7)	59.0 (17.3)
3	33	61.0 (15.6)	63.6	6.0 (0.9)	138.6 (169.4)	59.8 (22.1)
4	33	63.7 (15.9)	60.6	6.0 (0.7)	142.7 (143.2)	58.2 (16.1)
5	33	56.5 (18.1)	72.7	5.9 (0.8)	139.8 (169.0)	59.1 (21.0)
Overall	165	61.0 (16.5)	66.1	6.0 (1.0)	141.4 (167.7)	58.9 (20.2)

Group	Average insulin usage (U/h)	Average absolute goal feed (ml/h)	Average % goal feed (%)	Mortality (%)	APACHE II
1	2.6 (1.1)	75.3 (10.6)	48.3 (38.7)	72.7	20.5 (8.8)
2	2.6 (1.2)	73.0 (10.3)	52.0 (36.0)	81.8	17.7 (7.1)
3	2.6 (0.7)	74.7 (10.7)	52.5 (42.3)	84.8	20.9 (8.8)
4	2.7 (1.0)	70.9 (10.3)	54.0 (32.7)	87.9	21.3 (6.4)
5	2.5 (0.7)	77.3 (10.4)	52.7 (32.5)	82.4	20.5 (7.3)
Overall	2.6 (0.9)	74.2 (10.5)	51.9 (36.4)	81.9	20.2 (7.7)

insulin and dextrose infusions. The algorithm obeys the following rules in a prioritised order.

1. The lower bound of the equal-tailed 0.90 probability intervals in blood glucose levels resulted from control interventions must never be lower than 4 mmol/L.
2. The controller specified dextrose feeding rate must be greater than or equal to the patient specific minimum [6,12].
3. The total hourly insulin input must not exceed 6 U [10,38].
4. Saturation in Q (Eqs. (1) and (2)) must not exceed 200 mU/L:

$$Q - \frac{Q}{1 + \alpha_G Q} \leq 200 \, \text{mL/L} \tag{17}$$

5. The target blood glucose level (median of the blood glucose probability density function) is 85% of the blood glucose level at the time of intervention, to a minimum of 4.5 mmol/L.
6a. To lower blood glucose levels, the control algorithm seeks to lower the dextrose feeding rate before adding insulin in bolus (injection) form. Insulin infusions may be used to lower blood glucose levels without resulting in excess interstitial insulin saturation (rule 4).
6b. To increase low blood glucose levels, the control algorithm reduces insulin inputs first, and then increases dextrose rates.

The first 4 rules are designed for patient safety. If the target blood glucose level cannot be achieved without violating these first 4 rules, it is "bounded" so it can be achieved within these limitations. The final 3 rules define how the algorithm prioritises achieving the target blood glucose level.

4. Results and discussion

4.1. Cross validation

Table 3 shows the general information on the five patient groups used in cross validation.

The percentage of fitted S_I within the equal-tailed 0.90 and inter-quartile probability intervals for the group not used in creating the cross validation model is summarised in Table 4. Each group produced similar results, which were also comparable to the overall result. Thus, there is no significant difference between the 5 stochastic models created and the SPRINT cohort can be considered a generic representation of this ICU population.

More specifically, the mean per patient average of identified S_I values within the equal-tailed probability interval is 86.6%, and 54.0% for the inter-quartile interval. The equal tailed 0.90 probability interval slightly underestimates the identified S_I range, because when $S_{I,n}$ is close to its fitting constraints, the $S_{I,n+1}$ probability density function tends to peak near the boundary value. This behaviour causes some regions outside

Table 4 – Stochastic insulin sensitivity model cross validation results

Group	Groups used in creating stochastic model	Average percentage of fitted S_I within equal-tailed 0.90 probability interval (%)	Average percentage of fitted S_I within inter-quartile probability interval (%)
1	[–, 2, 3, 4, 5]	85.7	54.2
2	[1, –, 3, 4, 5]	83.2	52.3
3	[1, 2, –, 4, 5]	87.4	54.7
4	[1, 2, 3, –, 5]	88.7	54.1
5	[1, 2, 3, 4, –]	87.9	54.8
Overall	[1, 2, 3, 4, 5]	86.6	54.0

of the equal-tailed 0.90 probability intervals to have higher probability density than some regions within the interval, as shown in Figs. 3 and 5. Thus, the compromise of using equal-tailed probability intervals has negligible impact compared to the computational gain over calculating the exact blood glucose ranges of the highest 0.90 probability density.

The inter-quartile probability intervals include slightly over 50% of fitted S_I, suggesting that most of the time the higher probability density is concentrated about the median of the probability density functions, as also seen in Figs. 3 and 5. Similarly, the 0.90 probability interval has slightly less than 90% of all measurements, suggesting that there are slightly more outliers than represented in the model. Both results suggest that the assumptions used are slightly inexact, but within typical variations caused by the 7–12% measurement error [36,39].

4.2.   *Virtual control trial results*

A virtual cohort of 200 patients was created and tested in simulated trials. Blood glucose probability intervals from control inputs were produced with each control intervention using the stochastic model. Hourly blood glucose measurements includ-

ing normally distributed random measurement noise were analysed against the probability intervals. An example of a virtual trial is shown in Fig. 6. The top panel shows the blood glucose excursion through time. The bold crosses are the virtually generated blood glucose levels at one hour intervals, with thick bars indicating the standard 7% Glucocard™ measurement error [36]. Hourly S_I is shown in the bottom panel. Control interventions are determined hourly and shown in the middle panel, producing stochastic model derived probability median values and intervals in blood glucose shown as circles with thin bars in the top panel.

The average fractions of virtual trial blood glucose levels within the equal-tailed 0.90 and inter-quartile probability intervals for each patient are shown in Fig. 7. The logistic mean of percentage blood glucose levels within the equal-tailed 0.90 and inter-quartile probability interval are 87.0% and 45.7%, respectively. These results are in general agreement with the cross validation results in Table 5. These per patient results also show the overall validity in total, as well as over all virtual patients, with very few outlying virtual patients.

A few trials in Fig. 7 have comparatively lower percentages within the probability intervals. These trials are all shorter,
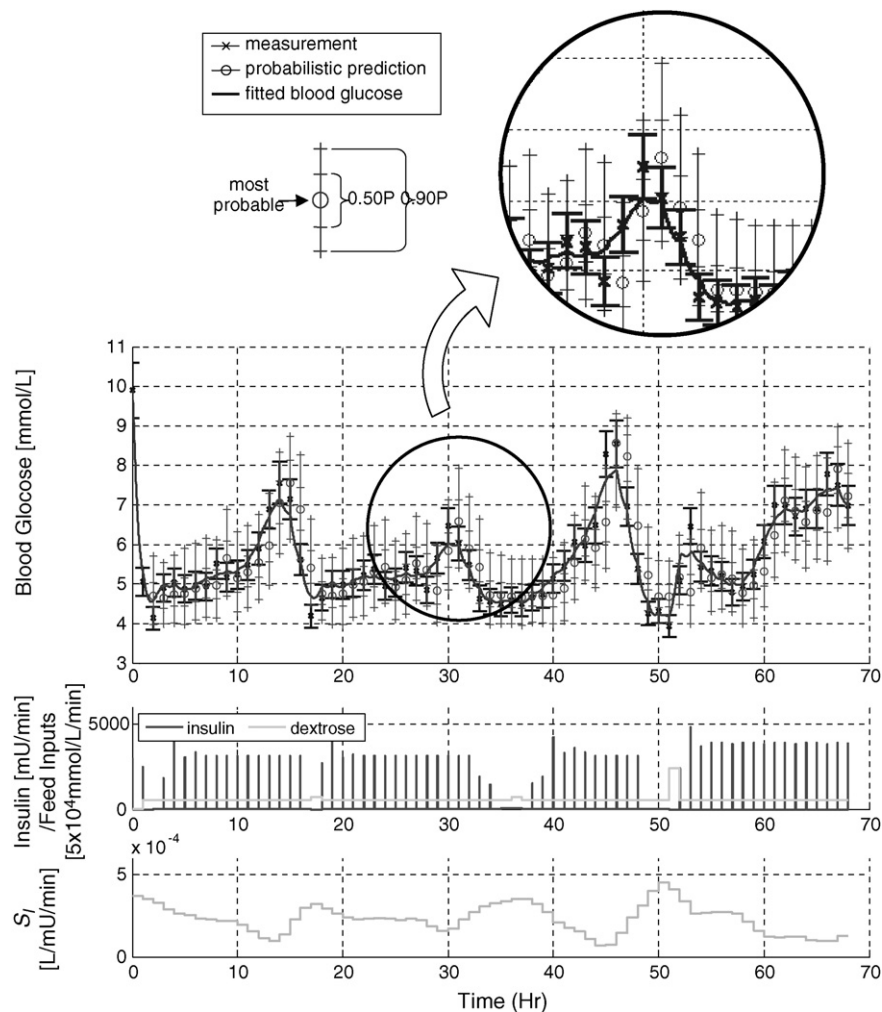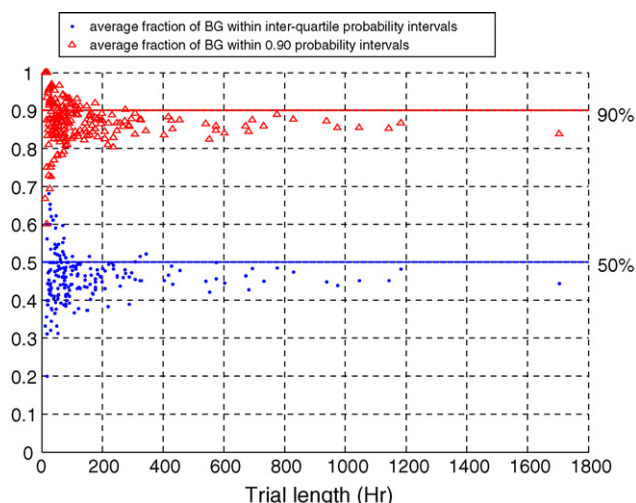

Fig. 6 – Example of a virtual trial. The top panel displays the blood glucose evolution, where bold crosses are virtually generated blood glucose levels are 1 h intervals, with thick bars indicating measurement error. The controller predicted blood glucose levels are shown in circles, with thin bars indicating their probability intervals.
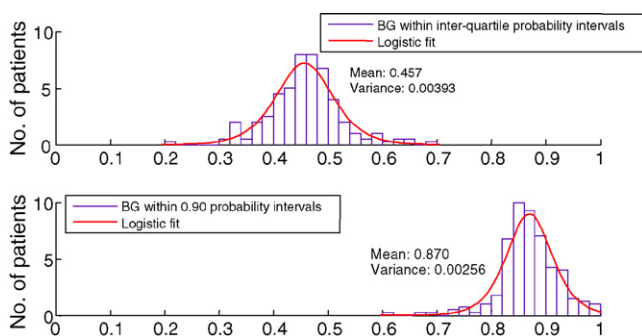
Fig. 7 – Probability interval analysis per patient. Plotted are the individual patient averages. The upper plot is the fraction of measurements in the inter-quartile interval. The bottom panel is the fraction in the 0.90 probability interval.

Fig. 8 – Virtual trial length versus probability interval accuracy.

and consequently a small number of blood glucose levels outside of the probability intervals are reported as higher percentages of the total. Fig. 8 illustrates how shorter trials can produce outliers, where most variability is gone after 50–75 h, indicating stabilised patient condition under long term, tight glycemic control with little variability in glycemic level. It also shows how as time length of trial increases, the 0.90 and inter-quartile probability intervals are both slightly conservative estimates by 2–4%, as also seen in the median values of Fig. 7.

The control algorithm used to run these virtual trials targets the blood glucose probability density medians to the desired level. The controller specified interventions should thus theoretically result in the median blood glucose level being at the desired level one hour later. The distribution of virtual trial deviations (percentage value) from the probability density medians is shown in Fig. 9. The mean per patient

average deviation is 8.84%, as compared to a normally distributed random measurement error of 7–10%. Outliers are again associated with shorter trial length.

Examining the signed blood glucose deviations from probabilistic medians, 58% are negative. This result suggests that slightly higher density may be concentrated at higher S_I in the probability density functions. In the future, this blood glucose deviation could be "corrected" for in the control algorithm by targeting a percentile higher than the 50th, for example the 58th percentile, until the deviation is minimised, thus further improving the targeting accuracy. Similar manipulation may also be carried out to "correct" the accuracy of the probability intervals.
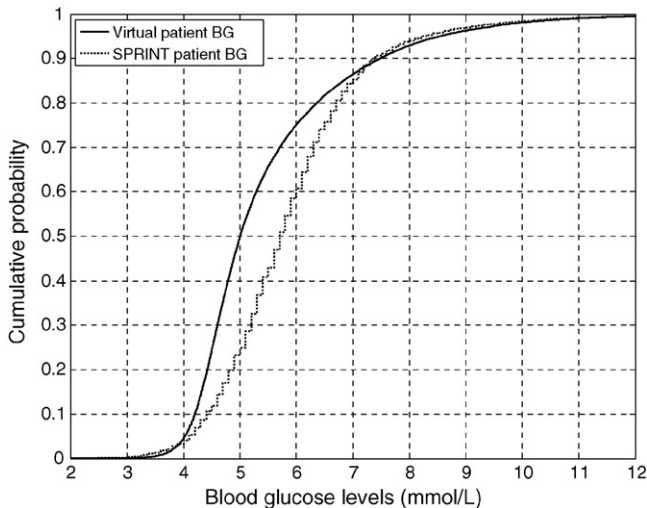
Table 5 – Virtual trial results compared to clinical SPRINT results		
	SPRINT	Virtual trials
Overall data		
Number of patients	165	200
Hours number of control (h)	23,324	33,889
Total BG measurements	15,874	34,089
BG mean[a] (mmol/L)	5.9 [4.1–8.3]	5.5 [3.6–7.8]
BG standard deviation[a] (mmol/L)	1.3	1.3
Percentage between 4 and 6.1 mmol/L (%)	61	72
Percentage between 4 and 7.0 mmol/L (%)	82	82
Percentage between 4 and 7.75 mmol/L (%)	89	87
Percentage <4 mmol/L (%)	3.3	4.5
Percentage <2.5 mmol/L (%)	0.1	0.02
Per-patient data		
Hours of control (h)	95 [12–447]	79 [20–688]
Number of measurements	68[10–271]	80[21–689]
BG mean (mmol/L)	5.9 [5.0–7.4]	5.3 [4.6–7.5]
BG standard deviation (mmol/L)	1.1 [0.7–2.3]	1.0 [0.5–2.1]
Median hourly insulin (U)	2.5[1.3–4.1]	3.2 [1.3–4.4]
Median nutrition rate (resource diabetic) (ml/h)	37.5 [0–80.3]	28.2 [18.1–42.9]
(Assuming 1.06 cal/ml) (kcal/day)	954 [0–2043]	717 [461–1093]
Median percentage of goal feed	52.7% [29.7–70.3%]	38.4% [29.3–67.6%]
[a] Lognormal distribution. Data are expressed as median [5–95th percentile range] as appropriate.		
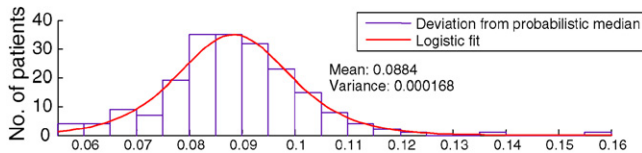
Fig. 9 – **Percentage deviation of virtual trial blood glucose levels from probabilistic medians.**

Fig. 10 – **Blood glucose measurement distribution comparison between clinical SPRINT results and virtual patients under the improved stochastic controller presented.**

Virtual trial controller performance is compared to the actual clinical SPRINT results and summarised in Table 5. The blood glucose is more tightly controlled, with a lower mean level (5.5 mmol/L versus 5.9 mmol/L), and a similar, but safer, 5–95th percentile interval ([4.1–8.3] versus [3.6–7.8]). The percentage of blood glucose in the 4–6 mmol/L range increases from 61% to 72%. Without the stochastic targeting, the effectively same control protocol delivered only 64% time in this band [6]. It is a significant difference as tighter control has been shown to imply a better mortality outcome [4]. Again, the control quality is linked with trial length. Shorter trials tend to give a sparser blood glucose distribution and higher variance. This was also seen in SPRINT where the cohort with length of stay <3 days had greater variability.

Finally, a similar comparison is shown in Fig. 10. The percentage lower than 4 mmol/L is slightly increased from 3.3% to 4.5%, with 0% under 2.5 mmol/L. The percentage lower than 4 mmol/L can be easily reduced by setting a higher percentile limit in Rule 1, and/or increasing the minimum target from 4.5 mmol/L to 4.8–5.0 mmol/L in Rule 5.

5. Conclusions

The stochastic model presented defines the probability density functions of blood glucose levels one hour following a known glycemic control intervention, and thus enables more knowledgeable and accurate prediction for glycemic control.

The model created from 165 SPRINT trial patients was cross validated, verifying the generality of the chosen cohort and the method used to create the stochastic model. The model was then used to create 200 virtual patients representative of hyperglycaemic ICU patients based on clinical SPRINT protocol results. A stochastically targeted control protocol was then tested through numerical simulations.

Both the cross validation and the virtual trial simulation results confirm that the stochastic model provides accurate probabilistic knowledge. The cross validation results show that the 0.90 and inter-quartile probability intervals provide a slightly conservative bound, but accurately capture the cohort. The virtual trials also show that a stochastically-driven computerised control method can outperform a simplified version of the same basic insulin and nutrition control protocol, demonstrating further benefits of this model and/or computer control in general. In summary, the stochastic glucose–insulin system model presented can effectively capture critical care patient behaviour, enhance glycemic control and create a virtual patient platform for further development.

REFERENCES

[1] J. Chase, G.M. Shaw, X.W. Wong, T. Lotz, J. Lin, C.E. Hann, Model-based glycaemic control in critical care—a review of the state of the possible, Biomed. Signal Process. Control 1 (1) (2006) 3–21.

[2] J.S. Krinsley, Association between hyperglycemia and increased hospital mortality in a heterogeneous population of critically ill patients, Mayo Clin. Proc. 78 (12) (2003) 1471–1478.

[3] G. Van den Berghe, P. Wouters, F. Weekers, C. Verwaest, F. Bruyninckx, M. Schetz, D. Vlasselaers, P. Ferdinande, P. Lauwers, R. Bouillon, Intensive insulin therapy in the critically ill patients, N. Engl. J. Med. 345 (19) (2001) 1359–1367.

[4] J.G. Chase, C.E. Hann, G.M. Shaw, X.W. Wong, J. Lin, T. Lotz, A.J. Le Compte, T. Lonergan, An overview of glycemic control in critical care—relating performance and clinical results, J. Diabetes Sci. Technol. 1 (1) (2006) 82–91, http://www.journalofdst.org.

[5] M. Turina, M. Christ-Crain, H.C. Polk Jr., Diabetes and hyperglycemia: strict glycemic control., Crit. Care Med. 34 (Suppl. 9) (2006) S291–S300.

[6] T. Lonergan, A. LeCompte, M. Willacy, J.G. Chase, G.M. Shaw, X.W. Wong, T. Lotz, J. Lin, C.E. Hann, A simple insulin-nutrition protocol for tight glycemic control in critical illness: development and protocol comparison, Diabetes Technol. Ther. 8 (2) (2006) 191–206.

[7] T. Lonergan, A. LeCompte, M. Willacy, J. Chase, G. Shaw, C. Hann, T. Lotz, J. Lin, X. Wong, A pilot study of the SPRINT protocol for tight glycaemic control in critically ill patients, Diabetes Technol. Ther. 84 (4) (2006) 449–462.

[8] J. Plank, J. Blaha, J. Cordingley, M.E. Wilinska, L.J. Chassin, C. Morgan, S. Squire, M. Haluzik, J. Kremen, S. Svacina, W. Toller, A. Plasnik, M. Ellmerer, R. Hovorka, T.R. Pieber, Multicentric, randomized, controlled trial to evaluate blood glucose control by the model predictive control algorithm versus routine glucose management protocols in intensive care unit patients, Diabetes Care 29 (2) (2006) 271–276.

[9] F. Chee, T.L. Fernando, A.V. Savkin, V. van Heeden, Expert PID control system for blood glucose control in critically ill patients, IEEE Trans. Inf. Technol. Biomed. 7 (4) (2003) 419–425.

[10] J.G. Chase, G.M. Shaw, J. Lin, C.V. Doran, C. Hann, M.B. Robertson, P.M. Browne, T. Lotz, G.C. Wake, B. Broughton, Adaptive bolus-based targeted glucose regulation of hyperglycaemia in critical care, Med. Eng. Phys. 27 (1) (2005) 1–11.

[11] J. Chase, G. Shaw, A. LeCompte, D. Lee, T. Lonergan, M. Willacy, X. Wong, J. Lin, T. Lotz, C. Hann, Tight glycaemic control in critical care using insulin and nutrition—the SPRINT protocol, in: Proceedings of the Sixth Annual Diabetes Technology Society Meeting, Diabetes Technology Society, Atlanta, GA, 2006.

[12] X.W. Wong, I. Singh-Levett, L.J. Hollingsworth, G.M. Shaw, C.E. Hann, T. Lotz, J. Lin, O.S. Wong, J.G. Chase, A novel, model-based insulin and nutrition delivery controller for glycemic regulation in critically ill patients, Diabetes Technol. Ther. 8 (2) (2006) 174–190.

[13] G. Van den Berghe, A. Wilmer, G. Hermans, W. Meersseman, P.J. Wouters, I. Milants, E. Van Wijngaerden, H. Bobbaers, R. Bouillon, Intensive insulin therapy in the medical ICU, N. Engl. J. Med. 354 (5) (2006) 449–461.

[14] T. Lonergan, A.L. Compte, M. Willacy, J.G. Chase, G.M. Shaw, C.E. Hann, T. Lotz, J. Lin, X.W. Wong, A pilot study of the SPRINT protocol for tight glycemic control in critically Ill patients, Diabetes Technol. Ther. 8 (4) (2006) 449–462.

[15] C.E. Hann, J.G. Chase, J. Lin, T. Lotz, C.V. Doran, G.M. Shaw, Integral-based parameter identification for long-term dynamic verification of a glucose–insulin system model, Comput. Methods Programs Biomed. 77 (3) (2005) 259–270.

[16] C. Hann, J. Chase, G. Shaw, Integral-based identification of patient specific parameters for a minimal cardiac model, Comput. Methods Programs Biomed. 81 (2) (2006) 181–192.

[17] T.F. Lotz, J.G. Chase, K.A. McAuley, G.M. Shaw, C.E. Hann, J.I. Mann, A highly correlated method to assess insulin resistance in broad populations, in: Proceedings of the 12th International Confon Biomedical Engineering (ICBME), Singapore, 2005.

[18] T. Lotz, J. Chase, K. McAuley, J. Lin, X. Wong, C. Hann, S. Andreassen, Integral-based identification of a physiological insulin and glucose model on euglycaemic clamp trials, in: Proceedings of the 14th IF AC Symposium on System Identification (SYSID 2006), Newcastle, Australia, 2006.

[19] T. Lotz, J. Chase, K. McAuley, D. Lee, J. Lin, C. Hann, J.I. Mann, Transient and steady state euglycemic clamp validation of a model for glycemic control and insulin sensitivity testing, Diabetes Technol. Ther. 8 (3) (2006) 338–346.

[20] E.R. Carson, C. Cobelli, Modelling methodology for physiology and medicine, in: Academic Press Series in Biomedical Engineering, Academic Press, San Diego, 2001, pp. xiv, 421.

[21] J. Lin, D.S. Lee, J.G. Chase, C.E. Hann, T. Lotz, X.W. Wong, Stochastic modelling of insulin sensitivity variability in critical care, Biomed. Signal Process. Control 1 (2006) 229–242.

[22] A. Natali, A. Gastaldelli, S. Camastra, A.M. Sironi, E. Toschi, A. Masoni, E. Ferrannini, A. Mari, Dose–response characteristics of insulin action on glucose metabolism: a non-steady-state approach, Am. J. Physiol. Endocrinol. Metab. 278 (5) (2000) E794–E801.

[23] R.L. Prigeon, M.E. Roder, D. Porte Jr., S.E. Kahn, The effect of insulin dose on the measurement of insulin sensitivity by the minimal model technique. Evidence for saturable insulin transport in humans, J. Clin. Invest. 97 (2) (1996) 501–507.

[24] D.W. Scott, Multivariate density estimation: theory, practice, and visualization, in: Wiley Series in Probability and Mathematical Statistics, John Wiley & Sons Inc., New York, 1992.

[25] E. Ferrannini, C. Cobelli, The kinetics of insulin in man. II. Role of the liver, Diabetes Metab. Rev. 3 (2) (1987) 365–397.

[26] R.S. Sherwin, K.J. Kramer, J.D. Tobin, P.A. Insel, J.E. Liljenquist, M. Berman, R. Andres, A model of the kinetics of insulin in man, J. Clin. Invest. 53 (5) (1974) 1481–1492.

[27] E. Ferrannini, A. Gastaldelli, Y. Miyazaki, M. Matsuda, A. Mari, R.A. DeFronzo, beta-Cell function in subjects spanning the range from normal glucose tolerance to overt diabetes: a new analysis, J. Clin. Endocrinol. Metab. 90 (1) (2005) 493–500.

[28] E. Van Cauter, F. Mestrez, J. Sturis, K.S. Polonsky, Estimation of insulin secretion rates from C-peptide levels. Comparison of individual and standard kinetic parameters for C-peptide clearance, Diabetes 41 (3) (1992) 368–377.

[29] K. Ellemann, B. Thorsteinsson, S. Fugleberg, B. Feldt-Rasmussen, O.O. Andersen, P. Gronbaek, C. Binder, Kinetics of insulin disappearance from plasma in cortisone-treated normal subjects, Clin. Endocrinol. (Oxford) 26 (5) (1987) 623–628.

[30] A. Thorell, O. Rooyackers, P. Myrenfors, M. Soop, J. Nygren, O.H. Ljungqvist, Intensive insulin treatment in critically ill trauma patients normalizes glucose by reducing endogenous glucose production, J. Clin. Endocrinol. Metab. 89 (11) (2004) 5382–5386.

[31] R.A. DeFronzo, J.D. Tobin, R. Andres, Glucose clamp technique: a method for quantifying insulin secretion and resistance, Am. J. Physiol. 237 (3) (1979) E214–E223.

[32] P.A. Insel, J.E. Liljenquist, J.D. Tobin, R.S. Sherwin, P. Watkins, R. Andres, M. Berman, Insulin control of glucose metabolism in man, J. Clin. Invest. 55 (5) (1975) 1057–1066.

[33] K. Transberg, P. Hagander, J. Thorell, Disappearance of insulin in man: variation with the plasma insulin level, Acta Endocrinol. (Copenh.) 97 (1981) 391–397.

[34] K.C. McCowen, A. Malhotra, B.R. Bistrian, Stress-induced hyperglycemia, Crit. Care Clin. 17 (1) (2001) 107–124.

[35] G. Casella, R.L. Berger, Distributions of functions of a random variable, in statistical inference, Duxbury (2002) 47–54.

[36] Arkray, Glucocard™ Test Strip 2 Data Sheet, Arkray Inc., Japan, 2001.

[37] X. Wong, J.G. Chase, G.M. Shaw, C. Hann, T. Lotz, J. Lin, I. Singh-Levett, L. Hollingsworth, O. Wong, S. Andreassen, Model predictive glycaemic regulation in critical illness using insulin and nutrition input: a pilot study, Med. Eng. Phys. 28 (7) (2006) 665–681.

[38] J.G. Chase, G.M. Shaw, J. Lin, C.V. Doran, M. Bloomfield, G.C. Wake, B. Broughton, C. Hann, T. Lotz, Impact of insulin-stimulated glucose removal saturation on dynamic modelling and control of hyperglycaemia, Int. J. Intell. Syst. Technol. Appl. (IJISTA) 1 (1/2) (2004) 79–94.

[39] T. Lotz, J.G. Chase, K. McAuley, G. Shaw, X.-W. Wong, J. Lin, A. Le Compte, C.E. Hann, J.I. Mann, Highly correlated model-based testing of insulin sensitivity—initial results for a proposed low-intensity test, in: Proceedings of the Sixth Annual Diabetes Technology Society Meeting, Atlanta, USA, 2006.